

GEOCHEMICAL EVALUATION OF SURFACE WATER QUALITY AND APPROPRIATENESS FOR DRINKING AND IRRIGATION PURPOSES IN THE AIN TAFARUT, GHADAMIS CITY, SW LIBYA

Osama R. Shaltami^{1*}, Fares F. Fares¹, Farag M. EL Oshebi¹, Hwedi Errishi², Fathi M. Salloum¹, Hafsa A. Alemam³, Abdurrahman A. Abulla³, Souad A. Moftah⁴, Rabea Elghazal⁵ and Mohamed Baayou⁶

¹Department of Earth Sciences, Faculty of Science, Benghazi University, Libya

²Department of Geography, Faculty of Arts, Benghazi University, Libya

³Biotechnology Research Center, Tripoli, Libya

⁴Department of zoology, Faculty of Science, Benghazi University, Libya

⁵Benghazi Children's Hospital, Libya

⁶Arabian Gulf Oil Company (AGOCO), Benghazi, Libya

*Corresponding Author:-

Abstract:-

The goal of the current study is the geochemical assessment of surface water at the Ain Tafariut, Ghadamis city, SW Libya. The chemical data include sulfur isotope ($\delta^{34}\text{S-SO}_4$), major ions, trace elements, EC, TDS, TH, Alk and pH. The water is immature and hard. It falls in the field between NaCl and NaCaHCO₃ types in the Piper diagram. Dominance of rock and evaporation is clear in the water. The contaminant values (except for Na, P, Cl, Br, Ba, Pb, As, Cd and Ni) are below the acceptable limit of WHO (2018). The water is seriously affected by P, Br and Ba (MI>6). The as content demonstrates that the water is not suitable for irrigation.

Keywords:- Geochemistry, Environmental Geochemistry, Water Quality, Drinking Water, Irrigation, Ain Tafariut, Ghadamis, Libya.

INTRODUCTION

The dramatic increase in the population of the globe makes it necessary to assess water sources, whether ground or surface water (e.g., Sudhakar and Narsimha, 2013; Flem *et al.*, 2018). The Ghadamis city is located in the Ghadamis Basin, SW Libya. The Ain Tafarut is far about 2km southwestern of the Ghadamis city (Fig. 1). The exposed rocks in the study LIBYA.1 area are mainly carbonates (limestone, dolomitic limestone and dolostone), with lesser amount of marl and gypsum. The age of these rocks is Late Cretaceous-Paleogene. Assessment of surface water in the Ain Tafarut for drinking and irrigation uses is the aim of the current study. As far as the authors believe that this work may be the first geochemical study of the Ain Tafarut, because we have not found a published work on this subject.

Climate

The study area is of an explicit desert nature with vegetation and settlements in small quantities. The temperature is high in the summer (33°C in average) and low in the winter. The climate can be categorized as hyper arid with fairly severe winter frost hazard.

Methodology

Four samples were collected from the studied water during January 2018. We took the samples from a depth of 15 cm below the water surface (the same method used in Shaltami *et al.*, 2017). Denver Instrument Model 50 was used to determine the electrical conductivity (EC), potential of hydrogen (pH) and Total Dissolved Solids (TDS). Cl, HCO₃ and SO₄ were measured by silver nitrate titration, acid-base titration and colorimetric-spectrophotometer, respectively. Ca, Mg, Na and K were determined by inductively coupled plasma-optical emission spectrometry (ICP-OES), and Mn, Si, Al, P, Fe, Ti and trace elements by inductively coupled plasma-mass spectrometry (ICP-MS). NO₃ and NH₃ were identified by ion chromatography and sulfur isotope ratios by Finnigan MAT-251 mass spectrometer. These analyses were done in the National Water Research Center, Ministry of Water Resources and Irrigation of Egypt.

Results and Discussion

The chemical analysis data of the studied water samples include pH, EC, TDS, sulfur isotope ($\delta^{34}\text{S-SO}_4$), major ions and trace elements (Table 1). Based on the TDS content, the Ain Tafarut is classified as brackish water.

Hydrochemistry

The average of the Cl/Na ratio in seawater (1.17) is slightly lower than that in the Ain Tafarut (1.30, in average). Figs (2-3) suggest that weathering of rocks and evaporation are dominant in the water. The weathering of carbonate rocks is evident from the high HCO₃/Cl ratio (1.63, in average). The Mg/Ca versus Na/Ca plot is also supported this interpretation (Fig. 4). Moreover, Fig (5) suggests that the source of sulfate in the Ain Tafarut is commonly attributed to the dissolution of gypsum and/or anhydrite in host rock.

We used the Na-K-Mg and Cl-SO₄-HCO₃ diagrams of Giggenbach (1988) to define the maturity of the studied water (Figs. 6-7). These diagrams denote that the water of the Ain Tafarut is immature. Furthermore, the pH versus Alk diagram of Singh and Hussian (2016) specifies that the samples is classified as hard water (Fig. 8).

The Schoeller, Stiff and Piper diagrams were used to assess the studied water (Figs. 9-10). The Schoeller diagram shows that the tendencies of cations and anions are Na>Ca>Mg>K and HCO₃+CO₃>Cl>SO₄, respectively. The Piper diagram points to mixed hydrochemical facies (NaCl-NaCaHCO₃ type). The Stiff diagram demonstrates the same result.

Saturation Index

According Piersanti *et al.*, (2017) the saturation index (SI) is calculated as:

$$\text{Log SI} = \log a_{\text{Ca}} + \log a_{\text{HCO}_3} + \log \text{Ks calcite}$$

$$\text{Log SI} = \log a_{\text{Ca}} + \log a_{\text{Mg}} + \log a_{\text{HCO}_3} + \log \text{Ks dolomite}$$

$$\text{Log SI} = \log a_{\text{Ca}} + \log a_{\text{SO}_4} + \log \text{Ks gypsum} \quad \text{Log SI} = \log a_{\text{Na}} + \log a_{\text{Cl}} + \log \text{Ks halite}$$

The Log SI is more than zero in all minerals, which indicate that the studied water is supersaturated with calcite, dolomite, gypsum and halite.

Drinking Water Quality

The total hardness (TH) and alkalinity (Alk) are calculated as:

$$\text{TH (mg/l CaCO}_3) = 2.5 \text{ Ca (mg/l)} + 4.1 \text{ Mg (mg/l)}$$

$$\text{Alk} = [\text{HCO}_3^-] + [\text{OH}^-] + 2[\text{CO}_3^{2-}]$$

In general, the contaminant values (except for Na, P, Cl, Br, Ba, Pb, As, Cd and Ni) in the studied water samples are below the permissible limit of WHO (2018, Table 2). The concentrations of Pb, As, Cd and Ni are about 2 times the WHO limit, while the Br and Ba contents are more than 14 and 32 times, respectively, than the acceptable limit.

Metal Index

The metal index (MI) is defined as: $\text{MI} = \text{C}/\text{MAC}$ (Caerio *et al.*, 2005). Where, C is the metal concentration (mg/l) and MAC (mg/l) is the acceptable limit of WHO (2018). Based on the purity, Caerio *et al.*, (2005) divided the metal index into six classes: very pure <0.3 (class I), pure 0.3-1 (class II), slightly affected 1-2 (class III), moderately affected 2-4 (class IV), strongly affected 4-6 (class V) and seriously affected >6 (class VI). The studied samples are very pure with K, Mg, Mn, Si, Li, B, Sn, Cu, Zn, Cr, V, Mo, Ag and U, pure with Ca, Al, Ti, F, Sr, Be, Bi, Se, Hg, Sb and Co, slightly

affected by Na and Pb, moderately affected by As, Cd and Ni, strongly affected by Fe and seriously affected by P, Br and Ba.

Irrigation Water Quality

To evaluate the irrigation water quality, we used the irrigation parameters such as pH, electrical conductivity (EC), sodium percent (Na %), sodium adsorption ratio (SAR), residue Sodium carbonate (RSC), magnesium adsorption ratio (MAR), Kelley's ratio (KR), lime deposition potential (LDP) and permeability index (PI) in addition to the concentration of trace elements. These parameters above are defined as:

$$\text{Na\%} = (\text{Na} \times 100) / (\text{Ca} + \text{Mg} + \text{Na} + \text{K})$$

$$\text{SAR} = \text{Na} / \sqrt{(\text{Ca} + \text{Mg}) / 2}$$

$$\text{RSC} = [\text{HCO}_3 + \text{CO}_3] - [\text{Ca} + \text{Mg}]$$

$$\text{MAR} = [\text{Mg} / (\text{Mg} + \text{Ca})] \times 100$$

$$\text{KR} = \text{Na} / (\text{Ca} + \text{Mg})$$

$$\text{LDP} = (\text{HCO}_3 + \text{CO}_3^{2-})$$

$$\text{PI} = [(\text{Na} + \text{HCO}_3) / (\text{Ca} + \text{Mg} + \text{Na})] \times 100$$

(All concentrations are expressed in meq/l)

Most irrigation parameters (pH = 7.7, Na% = 54.27, SAR = 6.77, RSC = -0.27, MAR = 32.83 and PI = 98.28) indicate that the studied water is suitable for irrigation. This supposition is supported by the concentration of most trace elements. The plot of EC (ds/m) versus Na% (Fig. 11) points to the good quality of the water. The high arsenic content refutes the above interpretation. In addition, the water displays high values of KR and LDP (1.21 and 7.62, respectively). The above argument suggests that the water of the Ain Tifarut is not appropriate for irrigation uses.

Conclusion

The present study deals with geochemical estimation of surface water of Ain Tifarut at the Ghadamis city, SW Libya. The allowed limit of WHO (2018) is over the analyzed pollutants (except for Na, P, Cl, Br, Ba, Pb, Hg, As, Cd and Ni). The MI values point to significant contamination by Na, Pb, As, Cd, Ni, Fe, P, Br and Ba. Weathering of carbonate rocks and evaporitic gypsum are prevalent in the Ain Tifarut. The detected water type is a mixed hydrochemical facies (NaCl-NaCaHCO₃ type). The Ain Tifarut is classified as Immature and hard water. Based on the Log SI values, the water is supersaturated with calcite, dolomite, gypsum and halite. The studied water is not fitting for irrigation due to the high concentration of As.

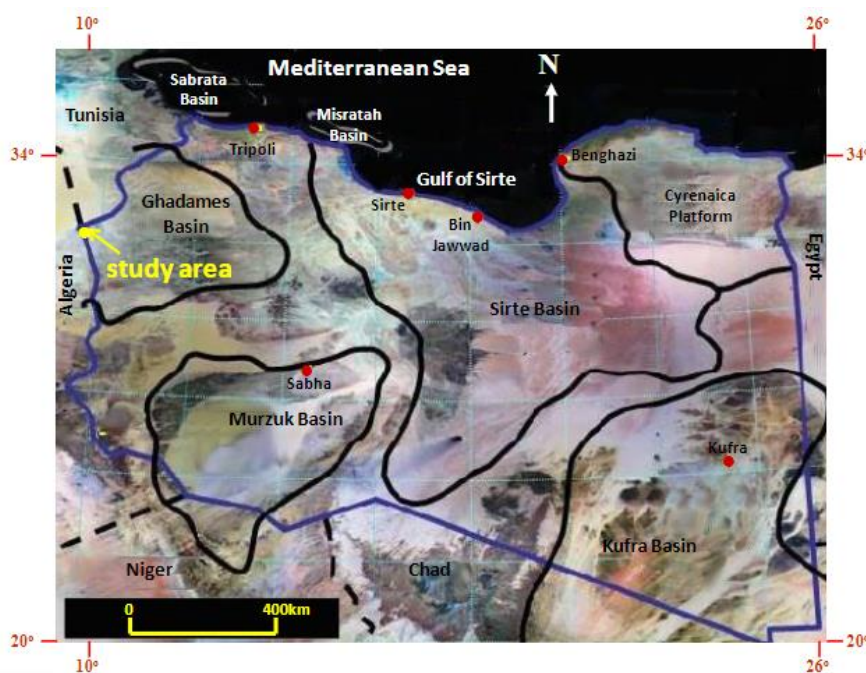


Fig. 1: Location map of the Ain Tifarut

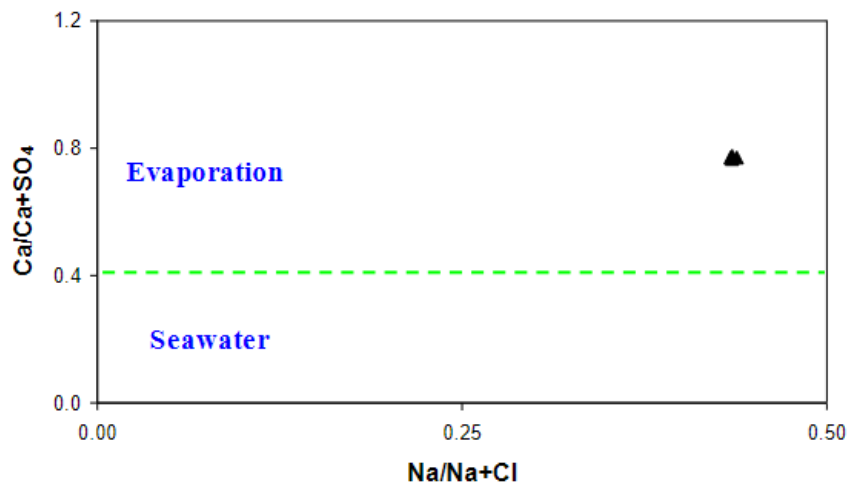


Fig. 2: Plot of $\text{Na}/(\text{Na}+\text{Cl})$ vs. $\text{Ca}/(\text{Ca}+\text{SO}_4)$ of the Ain Tafariut (fields after Hounslow, 1995)

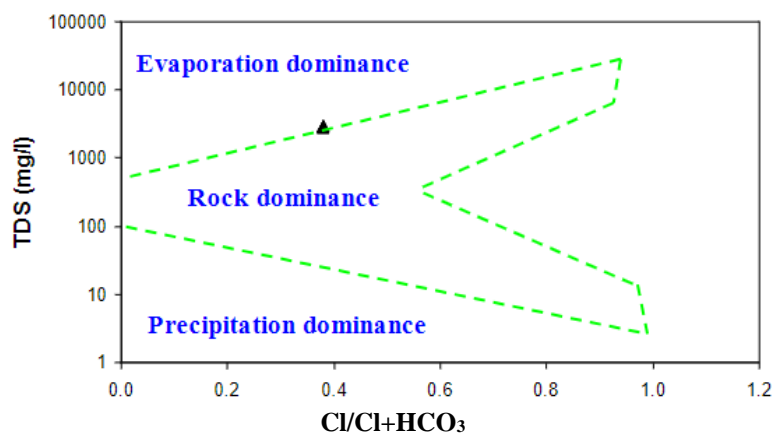


Fig. 3: Plot of $\text{Cl}/(\text{Cl}+\text{HCO}_3)$ vs. TDS (mg/l) of the Ain Tafariut (fields after Gibbs, 1970)

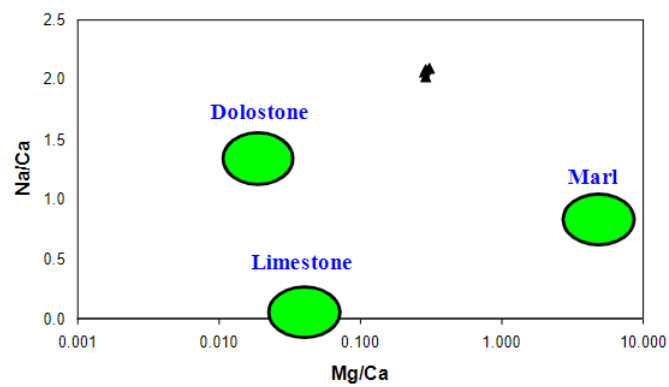


Fig. 4: Plot of Mg/Ca vs. Na/Ca of the Ain Tafariut (modified after Han and Liu, 2004)

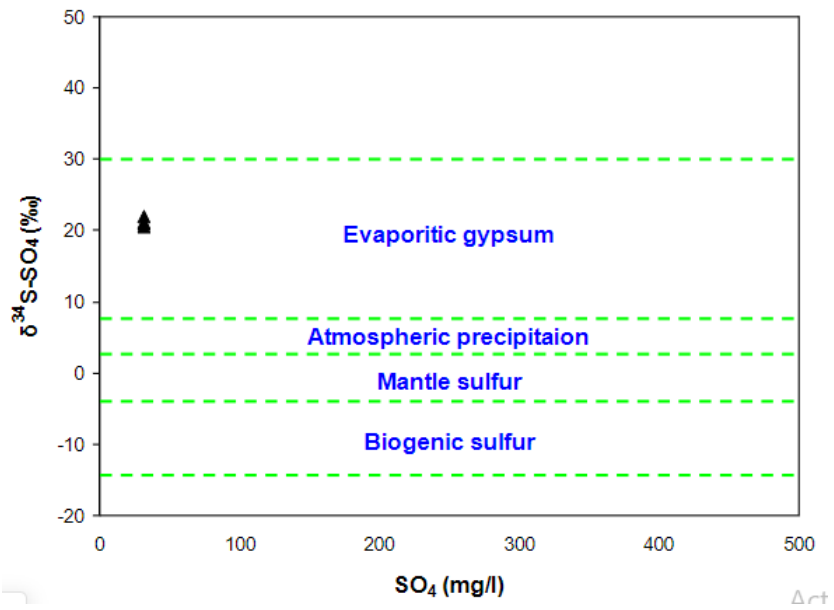


Fig. 5: Plot of SO_4 vs. $\delta^{34}\text{S-SO}_4$ of the Ain Tamarut (fields after Liu *et al.*, 2017)

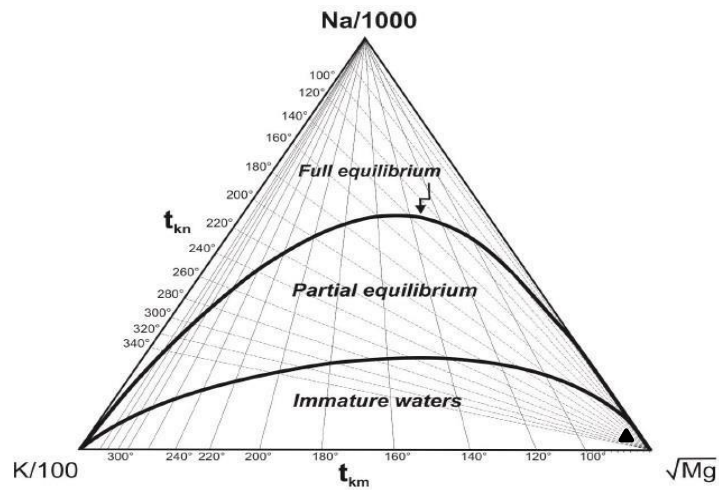


Fig. 6: Na-K-Mg diagram of the Ain Tamarut (fields after Giggenbach, 1988)

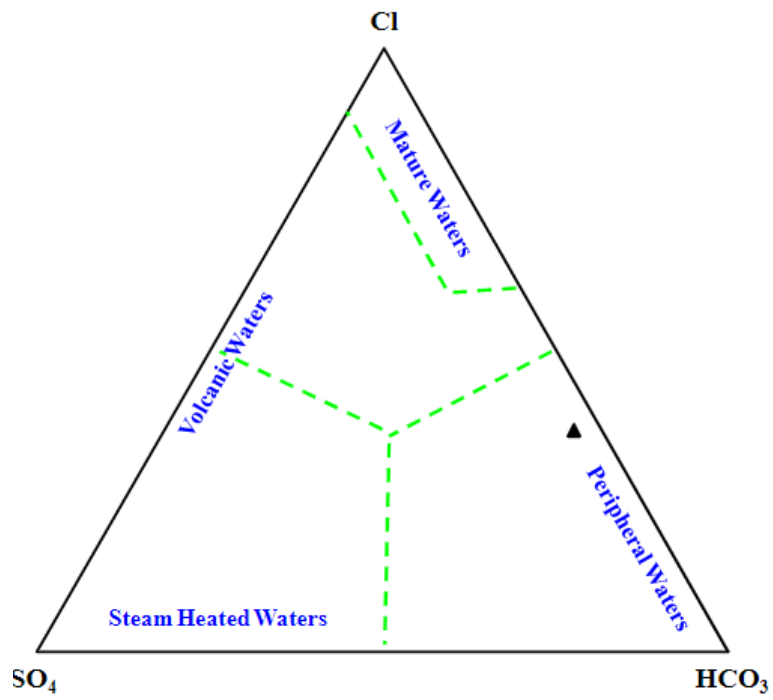


Fig. 7: Cl-SO₄-HCO₃ diagram of the Ain Tamarut (fields after Giggensch, 1988)

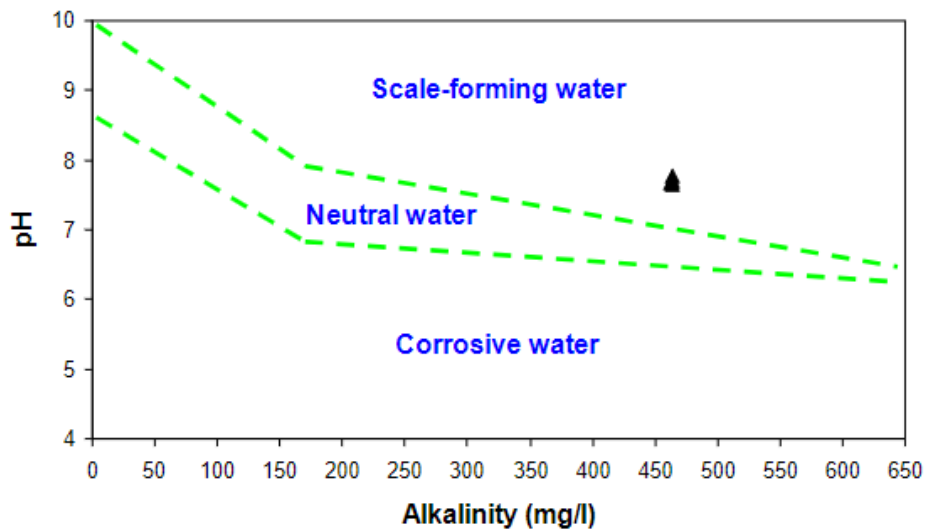


Fig. 8: Plot of pH vs. alkalinity of the Ain Tamarut (Fields after Singh and Hussian, 2016)

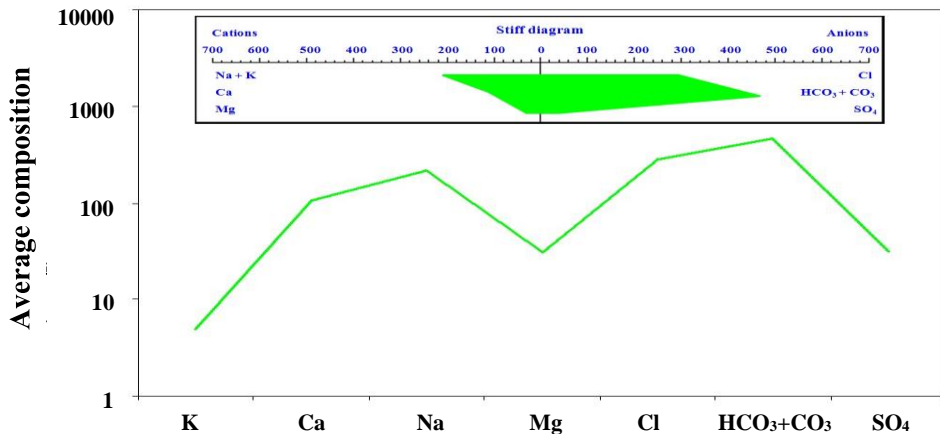


Fig. 9: Schoeller diagram of the Ain Tatarut. Stiff diagram is shown in inset

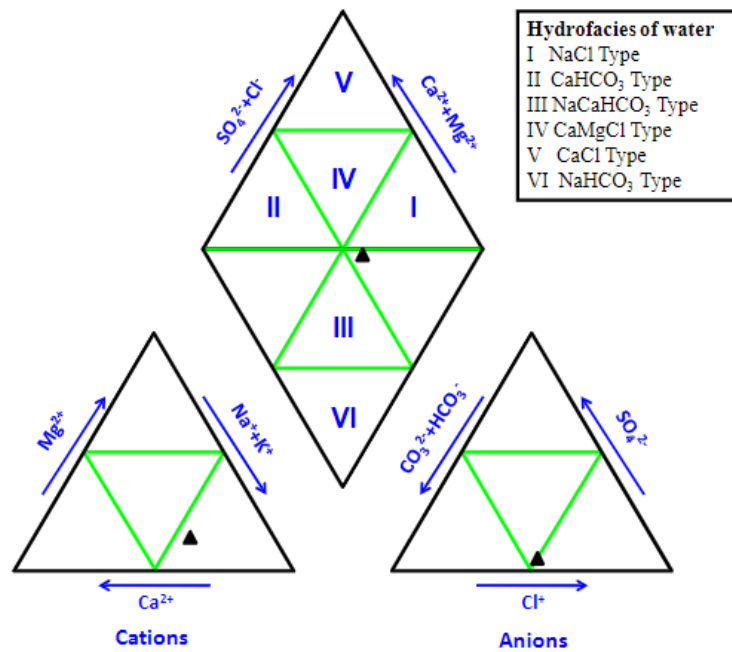


Fig. 10: Piper diagram of the Ain Tatarut (fields after Tweed *et al.*, 2005)

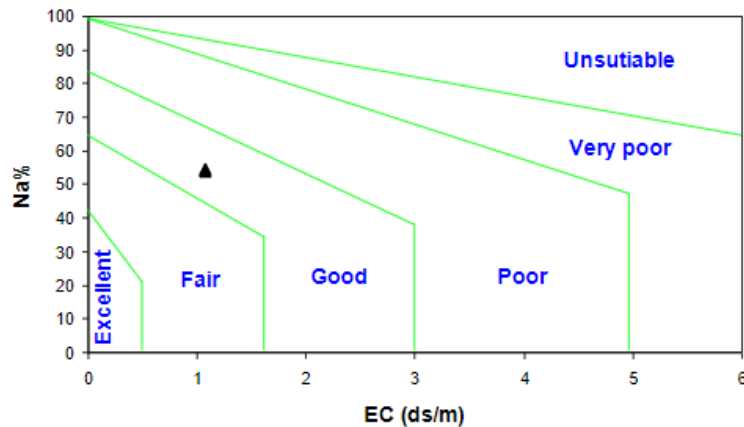


Fig. 11: Plot of EC vs. Na% of the Ain Tatarut (fields after Johnson and Zhang, 1990)

Table 1: Chemical analysis data (concentrations in mg/l, except for $\delta^{34}\text{S-SO}_4$ in ‰ and EC in $\mu\text{s/m}$) of the surface water of the Ain Tafariut

Parameters	1	2	3	4
pH	7.71	7.65	7.68	7.77
EC	1075	1077	1071	1070
K	4.55	5.00	4.59	5.51
Ca	107.80	104.64	104.61	106.79
Na	218.00	219.08	217.93	220.05
Mg	31.31	32.08	30.53	30.40
Mn	0.09	0.09	0.09	0.09
Si	6.25	7.12	6.19	7.31
Al	0.22	0.37	0.41	0.29
Fe	1.00	1.57	1.88	1.04
Ti	0.003	0.003	0.003	0.003
P	0.18	0.11	0.16	0.09
Cl	282.87	284.94	283.96	282.31
HCO ₃	463.50	463.54	462.15	462.44
SO ₄	31.25	32.17	31.20	31.89
$\delta^{34}\text{S-SO}_2$	20.86	21.21	20.56	22.00
NO ₃	0.91	0.98	0.89	0.92
NH ₃	0.27	0.32	0.39	0.25
TDS	2809	2903	2905	2904
F	0.90	0.82	0.95	0.90
Br	6.68	7.69	8.25	6.66
Li	0.05	0.05	0.05	0.05
Sr	1.23	1.16	1.40	1.42
Ba	0.11	0.20	0.24	0.10
Be	0.003	0.003	0.003	0.003
Bi	0.002	0.002	0.002	0.002
B	0.67	0.55	0.42	0.47
Se	0.04	0.04	0.04	0.04
Pb	0.02	0.02	0.02	0.02
Hg	0.0004	0.0004	0.0004	0.0004
As	0.20	0.29	0.22	0.24
Sn	0.004	0.004	0.004	0.004
Sb	0.003	0.003	0.003	0.003
Cd	0.005	0.005	0.005	0.005
Cu	0.02	0.02	0.02	0.02
Zn	0.04	0.04	0.04	0.04
Co	0.001	0.001	0.001	0.001
Cr	0.01	0.01	0.01	0.01
V	0.004	0.004	0.004	0.004
Ni	0.05	0.05	0.05	0.05
Mo	0.002	0.002	0.002	0.002
Ag	0.001	0.001	0.001	0.001
U	0.006	0.006	0.006	0.006

Table 2: Comparison between the chemical data of Ain Tafariut and the permissible limits of WHO (2018) for drinking water (concentrations in mg/l)

Contaminant	Sample No.				WHO
	1	2	3	4	
pH	7.71	7.65	7.68	7.77	8
K	4.55	5.00	4.59	5.51	100
Ca	107.80	104.64	104.61	106.79	200
Na	218.00	219.08	217.93	220.05	200
Mg	31.31	32.08	30.53	30.40	150
Mn	0.09	0.09	0.09	0.09	0.4
Si	6.25	7.12	6.19	7.31	28
Al	0.22	0.37	0.41	0.29	0.85
Fe	1.00	1.57	1.88	1.04	0.3
Ti	0.003	0.003	0.003	0.003	0.003
P	0.18	0.11	0.16	0.09	0.02
Cl	282.87	284.94	283.96	282.31	250
HCO ₃	463.50	463.54	462.15	462.44	600
SO ₄	31.25	32.17	31.20	31.89	600
NO ₃	0.91	0.98	0.89	0.92	10
NH ₃	0.27	0.32	0.39	0.25	0.5
TDS	2809	2903	2905	2904	500
TH	397.87	393.13	386.70	391.62	500
Alk	464.49	464.40	463.07	463.58	200
F	0.90	0.82	0.95	0.90	1.5
Br	6.68	7.69	8.25	6.66	0.5
Li	0.05	0.05	0.05	0.05	0.7
Sr	1.23	1.16	1.40	1.42	1.5
Ba	0.11	0.20	0.24	0.10	0.005
Be	0.003	0.003	0.003	0.003	0.004
Bi	0.002	0.002	0.002	0.002	0.004
B	0.67	0.55	0.42	0.47	2

Se	0.04	0.04	0.04	0.04	0.05
Pb	0.02	0.02	0.02	0.02	0.01
Hg	0.0004	0.0004	0.0004	0.0004	0.001
As	0.20	0.29	0.22	0.24	0.1
Sn	0.004	0.004	0.004	0.004	0.3
Sb	0.003	0.003	0.003	0.003	0.006
Cd	0.005	0.005	0.005	0.005	0.002
Cu	0.02	0.02	0.02	0.02	2
Zn	0.04	0.04	0.04	0.04	3
Co	0.001	0.001	0.001	0.001	0.002
Cr	0.01	0.01	0.01	0.01	0.05
V	0.004	0.004	0.004	0.004	0.14
Ni	0.05	0.05	0.05	0.05	0.02
Mo	0.002	0.002	0.002	0.002	0.02
Ag	0.001	0.001	0.001	0.001	0.1
U	0.006	0.006	0.006	0.006	0.03

References

- [1].Caerio, S., Costa, M.H., Ramos, T.B., Fernandes, F., Silveira, N., Coimbra, A. and Painho, M. (2005): Assessing heavy metal contamination in Sado Estuary sediment: An index analysis approach. *Ecological Indicators*; 5: 155-169.
- [2].Flem, B., Reimann, C., Fabian, K., Birke, M., Filzmoser, P. and Banks, D. (2018): Graphical statistics to explore the natural and anthropogenic processes influencing the inorganic quality of drinking water, ground water and surface water. *Applied Geochemistry*; 88: 133-148.
- [3].Gibbs, R.J. (1970): Mechanisms controlling world water chemistry. *Science*; 170: 10881090.
- [4].Giggenbach, W. (1988): Geothermal solute equilibria. Derivation of Na-K-Mg-Ca Geoindicators. *Geochimica et Cosmochimica Acta*; 55: 2749-2765.
- [5].Han, G. and Liu, C.Q. (2004): Water geochemistry controlled by carbonate dissolution: a study of the river waters draining karst-dominated terrain, Guizhou Province, China.
- [6].*Chemical Geology*; 204: 1-21.
- [7].Hounslow, A.W. (1995): *Water quality data: Analysis and interpretation*. Lewis Pub., New York, 397p.
- [8].Johnson, G. and Zhang, H. (1990): Classification of irrigation water quality, Oklahoma cooperative extension fact sheets (available at <http://www.osuextra.com>).
- [9].Liu, M., Guo, Q., Zhang, C., Zhu, M. and Li, J. (2017): Sulfur isotope geochemistry indicating the source of dissolved sulfate in Gonghe geothermal waters, northwestern China.
- [10].*Procedia Earth and Planetary Science*; 17: 157-160.
- [11].Piersanti, S., Shaltami, O.R., Fares, F.F., Salloum, F.M. and Muftah, A.M. (2017): Geochemistry of surface coastal water along the Mediterranean Coast from Tolmeita to Al Kuwifia, NE Libya. *Venice 1st International Conference on Engineering and Technology*,
- [12]. *Computer, Basic and Applied Sciences (ECBA- 2017)*, Venice, Italy, Proceeding Book; pp. 111-129.
- [13]. Shaltami, O.R., Fares, F.F., Salloum, F.M., Elghazal, R. and El Feituri, M.A. (2017):
- [14]. Assessment of surface water quality for drinking and irrigation purposes in Ain Apollo, Shahat city, NE Libya. 2nd Libyan Conference on Chemistry and its Applications (LCCA-2), Benghazi, Libya, Proceeding Book; pp. 127-134.
- [15]. Singh, S. and Hussian, A. (2016): Water quality index development for groundwater quality assessment of Greater Noida sub-basin, Uttar Pradesh, India. *Cogent Engineering*; 3: 1-17.
- [16]. Sudhakar, A. and Narsimha, A. (2013): Suitability and assessment of groundwater for irrigation purpose: A case study of Kushaiguda area, Ranga Reddy district, Andhra Pradesh, India. *Advances in Applied Science Research*; 4(6): 75-81.
- [17]. Tweed, S.O., Weaver, T.R. and Cartwright, I. (2005): Distinguishing groundwater flow paths in different fractured-rock aquifers using groundwater chemistry: Dandenong Ranges, Southeast Australia. *Hydrogeology Journal*; 13: 771-786.
- [18]. WHO (2018): Edition of the drinking water standards and health advisories Tables. EPA 822-F-18-001, Office of Water, U.S. Environmental Protection Agency Washington, DC; 12p. Faculty Of Science, Omar El –Mukhtar University El-Beida